Chalcogenide Letters Vol. 14, No. 6, June 2017, p. 217 - 221

SYNTHESIS AND OPTICAL PROPERTIES OF $Cu_2(Zn_{1-x}Mn_x)SnS_4$ THIN FILMS WITH TUNABLE BAND GAP

H. GUAN, H. SHEN*, J. LI
College of Materials Science and Technology, Nanjing University of Aeronautics and Astronautics, 29 Yudao Street, Nanjing 210016, PR China
2 School of Materials Engineering, Yancheng Institute of Technology, 9 Yinbing Street, Yancheng 224051, PR China

$Cu_2(Zn_{1-x}Mn_x)SnS_4$ thin films were one-step synthesized by a solvothermal method. The analytical results from XRD, Raman and SEM indicated that pure CZTS phase was obtained. By adjusting *x* values, the band gap of the $Cu_2(Zn_{1-x}Mn_x)SnS_4$ could be accordingly tailored from 1.18eV to 1.48eV.

(Received March 17, 2017; Accepted June 12, 2017)

Keywords: Solar cell materials, $Cu_2(Zn_{1-x}Mn_x)SnS_4$ thin films, Solvothermal method, Optical properties

1. Introduction

In recent years, the energy crisis makes people give great concern over thin film solar cells. As a promising absorber layer material, chalcopyrite semiconductor Cu_2ZnSnS_4(CZTS) are of great interest due to a suitable band-gap of around 1.5eV and high optical absorption coefficient beyond 10^4 cm^{-1}[1]. Compared with other chalcopyrite semiconductors such as Cu(In, Ga)Se_2, $CuSbSe_2$, CdTe etc, CZTS has good application potential owing to the composition of earth abundant and non-toxic elements. The power conversion efficiency of solar cells based on pure Cu_2ZnSnS_4 as high as 8.4% has been reported [2]. But the power conversion efficiency can be improved further because it is far behind the physical Shockley-Queisser limit of conversion efficiency (~31%)[3].

Various methods have been employed to synthesize CZTS thin films, such as sputtering, thermal evaporation, spray-pyrolysis, electrodeposition, sol-gel, chemical bath deposition, successive ionic layer absorption and reaction, solvothermal synthesis[4-19]. Among them, the solvothermal method has a number of advantages. Firstly, the chemical compositions can be readily controlled in a closed environment. Secondly, the size-uniformity and structural homogeneity can be improved. To date, the solvothermal method has been mainly employed to prepare CZTS nanocrystals. There is some literature on synthesizing CZTS thin films directly via a solvothermal method. As far as we know, no reports have been found to synthesize doped-type CZTS thin films directly by solvothermal method.

The optical and electrical properties can be optimized by varying stoichiometry and structure of CZTS. Chen revealed that the band gap of $Cu_2ZnSn(S, Se)_4$ is tuned from 1.0eV to 1.5eV by partly substituting S with Se[20]. Barkhouse fabricated $Cu_2ZnSn(S, Se)_4$ solar cells, exhibiting a power efficiencies as high as 10.1%[21]. The power efficiencies as high as 8.4% has been obtained by partly Ge replacing Sn[22]. Unfortunately, the Se and Ge are still unfriendly and rare. Therefore, other elements such as Fe, Mn, Co, Ni attract more and more attention because of their similar structures of Cu_2ZnSnS_4, Cu_2FeSnS_4, Cu_2MnSnS_4, Cu_2CoSnS_4 and Cu_2NiSnS_4. A few

*Corresponding author: hlshenktz@163.com

studies have been reported [23-24]. However, there exists a discrepancy about the band gap depending on the composition due to synthetic methods.

In this paper, $Cu_2(Zn_{1-x}Mn_x)SnS_4$ thin films were one-step synthesized by solvothermal method. The composition dependence of the structure and optical properties were studied.

2. Experimental details

Before depositing the $Cu_2(Zn_{1-x}Mn_x)SnS_4$ thin films, the glass substrates were firstly ultrasonically cleaned by cleaning powder, acetone, alcohol and de-ionized water for 10min, respectively. $Cu(NO_3)_2 \cdot 3H_2O$ (Analytical Reagent, Nanshi-Reagent), $Zn(CH_3COO)_2 \cdot 2H_2O$ (Analytical Reagent, Nanshi-Reagent), $Mn(CH_3COO)_2 \cdot 2H_2O$ (Analytical Reagent, Nanshi-Reagent), $SnCl_2 \cdot 2H_2O$ (Analytical Reagent, Nanshi-Reagent) and H_2NCSNH_2 (Analytical Reagent, Nanshi-Reagent) were used without any further purification. In a typical synthesis process, $Cu(NO_3)_2 \cdot 3H_2O$, $Zn(CH_3COO)_2 \cdot 2H_2O$, $Mn(CH_3COO)_2 \cdot 2H_2O$, $SnCl_2 \cdot 2H_2O$, H_2NCSNH_2 as raw materials in the proportion of 2:1-*x*:*x*:4(*x*=0, 0.3, 0.5, 0.7,1) were added in 40ml ethylene glycol under stirring for 40min at 45℃ as the precursor solution. Then the precursor solution was placed in a 50ml Teflon liner, and the well-cleaned glass substrates were immersed in it. The autocave was sealed and maintained at 200℃ for 24h. Thereafter, the autocave was cooled down to room temperature. The glass substrates were then rinsed with de-ionized water and subsequently dried.

The structure studies were carried out using a PANalytical X'Pert PRO diffractometer with Cu *Kα* radiation (λ=0.15406nm) and JY-T64000 Raman spectrometers. The microstructure was characterized by LEO-1530VP scanning electron microscope. The optical characteristics were measured using Varian Cary 5000 spectrophotometer to calculate band gap energy.

3. Results and discussion

In order to ensure pure CZTS thin film can be obtained under process conditions above, CZTS thin film was studied firstly. The XRD pattern of the CZTS thin film is shown in Fig.1(a). It can be seen that the diffraction peaks at 2θ=28.34°, 33.42°, 47.52° and 56.23° can be attributed to (112), (200), (220), (312), respectively. The plane shows the broad full-width at half-maxima (FWHM), indicating the formation of nanocrystallinity. The average grain size calculated using Debye-Scherrer is 4.37nm. The micro-strain (ε) and dislocation density (ρ) from 2θ and FWHM (β) of the related peaks are about 0.45 and 5.6×10^{16} m^{-2}, respectively. The structure of the CZTS thin film was further investigated by Raman spectrum due to their similar structure of kesterite CZTS, Cu_2SnS_3 and ZnS. Fig1(b) shows the Raman spectrum of the CZTS thin film. A strong peak at 337cm^{-1} corresponding to a kesterite CZTS is observed. There are no additional peaks for other phases, such as ZnS and Cu_2SnS_3, are observed, exhibiting the single phase of the CZTS thin film. It is concluded that the process parameters are proper. Fig.1(c) shows that the SEM images of the CZTS thin film. It can be seen that the CZTS thin film is composed of a large number of sphere-like particles, and the average size is about 500nm.

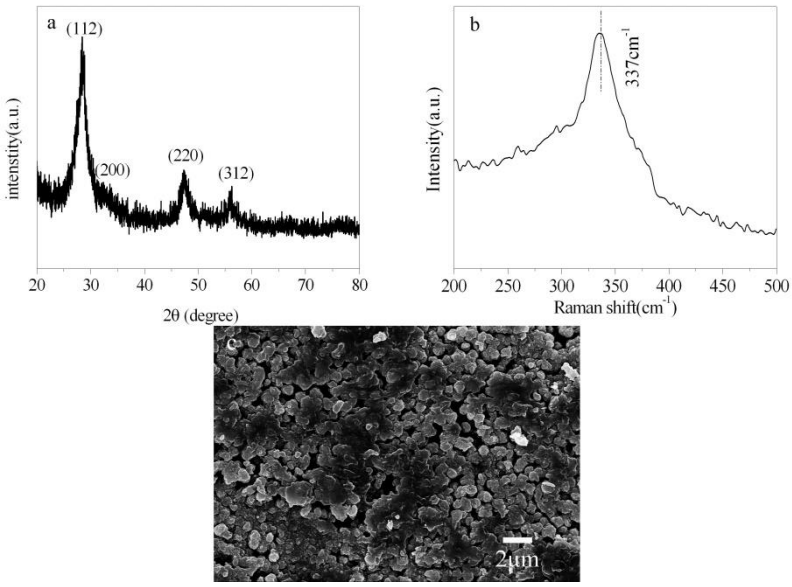

Fig.1 XRD pattern, Raman srectrum and SEM image of CZTS thin film

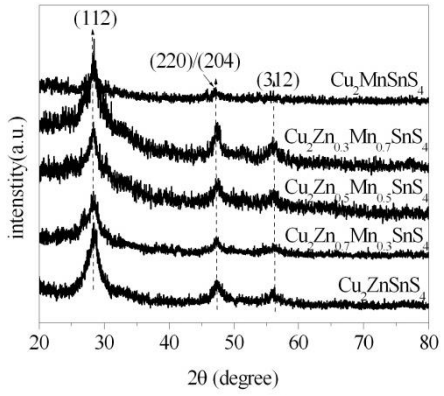

Fig.2 XRD patterns of $Cu_2(Zn_{1-x}Mn_x)SnS_4$ (x=0, 0.3, 0.5, 0.7,1) thin films

$Cu_2(Zn_{1-x}Mn_x)SnS_4$ thin films were synthesized under the same conditions, and the XRD patterns of the ones with different Mn compositions are shown in Fig.2. It is observed that the kesterite structure of CZTS(x=0) was obtained while the stannite structure of CMTS(x=1), which correspond to JCPDS 26-0575(CZTS) and JCPDS 51-0757 (CMTS), respectively. No impurity phase peaks are observed from all samples, indicating the high purity phase of $Cu_2(Zn_{1-x}Mn_x)SnS_4$ (x=0, 0.3, 0.5, 0.7,1) thin films. Moreover, we can investigate that the major peaks of $Cu_2(Zn_{1-x}Mn_x)SnS_4$ thin films shift toward the smaller angle with Mn gradually substituting for Zn, which results from the lattice extension due to the small radius of Zn cations (r_{Zn2+}=0.074nm) being replaced by the large radius of Zn cations (r_{Mn2+}=0.080nm)[23].

Fig.3 shows the SEM images of the $Cu_2(Zn_{1-x}Mn_x)SnS_4$ (x=0, 0.3, 0.5, 0.7,1) thin films. It can be seen that CZTS, $Cu_2Zn_{0.3}Mn_{0.7}SnS_4$ and CMTS are composed of sphere-like particles with different sizes whereas $Cu_2Zn_{0.7}Mn_{0.3}SnS_4$ and $Cu_2Zn_{0.5}Mn_{0.5}SnS_4$ show irregular particles. In particular, $Cu_2Zn_{0.7}Mn_{0.3}SnS_4$ thin film appears to be quite dense, which is benifical to improving the photovoltaic conversion efficiency.

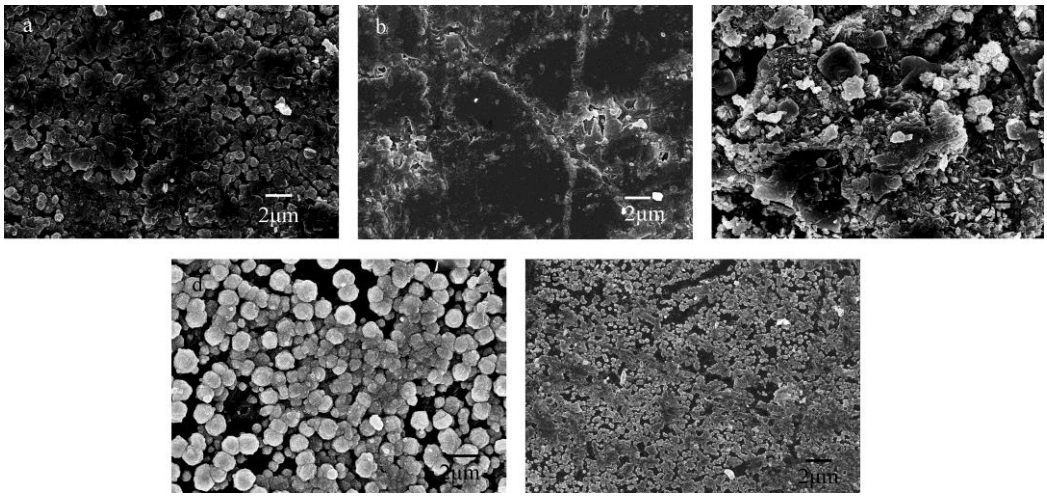

Fig. 3 SEM images of $Cu_2(Zn_{1-x}Mn_x)SnS_4$ (x=0, 0.3, 0.5, 0.7,1) thin films

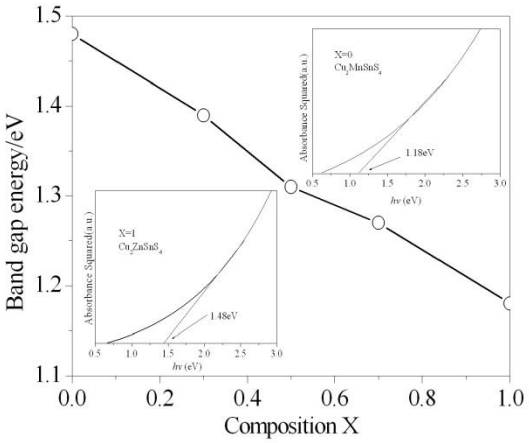

Fig. 4 The band gap as a function of x values
Inset: Plot of absorbsnce squared versus hv of CZTS and CMTS thin films

Fig.4 shows the results of optical band gap as a function of different *x* values. The optical band gap(E_g) of CZTS and CMTS thin films were obtained by extrapolating the linear absorption edge part of curve to the intersection with energy axis as shown in the insert. The estimated E_g values of $Cu_2(Zn_{1-x}Mn_x)SnS_4$ thin films are 1.48eV, 1.39eV, 1.31eV, 1.27eV and 1.18eV at x=0, 0.3, 0.5, 0.7 and 1, respectively, exhibiting suitable band gaps of the absorber materials for the thin solar cells. Furthermore, quasi-linear relationship between the band gap and *x* value obeys Vegard's law[24]. Therefore, the band gap of CZTS thin films can be tuned by Mn replacing Zn.

4. Conclusions

In this paper, we have successfully one-step synthesized $Cu_2(Zn_{1-x}Mn_x)SnS_4$ thin films by a solvothermal method. The analytical results from XRD, Raman and SEM indicate that pure CZTS phase was obtained at 200℃ for 24h. By adjusting *x* values, the band gap of the

$Cu_2(Zn_{1-x}Mn_x)SnS_4$ can be tuned from 1.18eV to 1.48eV. It is believed that $Cu_2(Zn_{1-x}Mn_x)SnS_4$ thin films with tunable band gap were obtained, and it is an application opportunity for the effective band engineering.

References

[1] S. W. Shin, S. M. Pawar, C. Y. Park, J. H. Yun, J. H. Moon, J. H. Kim, J. Y. Lee, Sol. Energy Mater. Sol. Cells **95**, 3202 (2011)
[2] B. Shin, O. Gunawan, Y. Zhu, N. A. Bojarczuk, S. J. Chey, S. Guha, Prog. Photovolt: Res. Appl. **21**, 72 (2011)
[3] W. Shockley, H. J. Queisser, J. Appl. Phys. **32**, 510 (1961)
[4] S. W. Fu, H. J. Chen, S. H. Wu, H. T. Wu, C. F. Shih, Mater. Lett. **173**, 1 (2016)
[5] T. Kubart, T. Ericson, J.J. Scragg, M. Edoff, C. Platzer-Björkman, Surf. Coatings Technol. **240**, 281 (2014)
[6] H. Nozaki, T. Fukano, S. Ohta, Y. Seno, H. Katagiri, K. Jimbo, J. Alloys Compd. **524**, 22 (2012)
[7] P. A. Fernandes , P. M. P. Salome ,A. F. D. Cunha, Thin Solid Films **517**, 2519 (2009)
[8] F. Q. Zeng , Y. Q. Lai, Z. L. Han, B. K. Ng, Z. A. Zhang, H. L. Zhang, L. X. Jiang, F. Y. Liu, RSC Adv. **6**, 6562 (2016)
[9] Z. Su, J. M. R. Tan, X. Li, X. Zeng, S. K. Batabyal, L. H. Wong, Adv. Energy Mater. **5**, 19 (2015)
[10] C. Gao, T. Schnabel, T. Abzieher, E. Ahlswede, M. Powalla, M. Hetterich, Appl. Phys. Lett. **108**, 013901 (2016)
[11] K. Tanaka, M. Oonuki, N. Moritake, H. Uchiki, Sol. Energy Mater. Sol. Cells **93**, 583 (2009)
[12] B. Long, S. Cheng, Y. Lai, H. Zhou, J. Yu, Q. Zheng, Thin Solid Films **573**, 117 (2014)
[13] J. Tao, K. Zhang, C. Zhang, L. Chen, H. Cao, J. Liu, J. Jiang, L. Sun, P. Yang, J. Chu, Chem. Commun. **51**, 10337 (2015)
[14] J. Tao, J. Liu, L. Chen, H. Cao, X. Meng, Y. Zhang, C. Zhang, L. Sun, P. Yang, J. Chu, Green Chem. **18**, 550 (2015)
[15] M. I. Khalil, R. Bernasconi, S. Ieffa, A. Lucotti, A. L. Donne, S. Binetti, L. Magagnin, ECS Transactions **64**, 33 (2015)
[16] N. M. Shinde, D. P. Dubal, D. S. Dhawale, C. D. Lokhande, J. H. Kim, J. H. Moon, Mater. Res. Bull. **47**, 302 (2012)
[17] S. S. Mali, P. S. Shinde, C. A. Betty, P. N. Bhosale, Y. W. Oh, P. S. Patil, J. Phys. Chem. Solid **73**, 735 (2012)
[18] S. S. Mali, P. S. Shinde, C. A. Betty, P. N. Bhosale, Y. W. Oh, S. R. Jadkar, R. S. Devan, Y. R. Ma, P. S. Patil, Electrochim. Acta **66**, 216 (2102)
[19] X. Yan, X. Hu, S. Komarneni, J. Korean Phys. Soc. **66**, 1511 (2015)
[20] S. Chen, A. Walsh, J. H. Yang, X.G. Gong, L. Sun, Phys. Rev. B:Condens. Matter **83**, 113 (2011)
[21] D. A. R. Barkhouse, O. Gunawan, T. Gokmen, T. K. Todorov, D. B. Mitzi, Prog. Photovolt: Res. Appl. **20**, 6 (2012)
[22] Q. Guo, G. M. Ford, W. C. Yang, C. J. Hages, H. W. Hillhouse, R. Agrawal, Sol. Energy Mater. Sol. Cells **105**, 132 (2012)
[23] L. Chen, H. Deng, J. Cui, J. Tao, W. Zhou, J. Alloy Compd. **627**, 388 (2015)
[24] Y. Xie, C. Zhang, G. Yang, J. Yang, X. Zhou, J. Ma, J. Alloy Compd. **696**, 938 (2016)